Isolation of Mouse Myocardial Gap Junctions

ROBERT W. KENSLER and DANIEL A. GOODENOUGH
Department of Anatomy, Harvard Medical School, Boston, Massachusetts 02115. Dr. Kensler's present address is the Department of Anatomy, Medical College of Pennsylvania, Philadelphia, Pennsylvania 19129.

ABSTRACT A new method is presented for the isolation of an enriched fraction of mouse myocardial gap junctions without the use of exogenous proteases. The junctions appear well preserved morphologically and similar to their appearance *in situ*. Contaminants of the preparation include fragments of the *fascia adherens* region of the intercalated disk. SDS polyacrylamide gel electrophoresis of the preparation reveals seven major bands with apparent mol wt of 28,000; 31,000; 33,500; 43,000; 47,000; 49,000; and 57,000. Only the bands at 38,000; 31,000; 33,500; and possibly the diffuse band at 47,000 copurify with the morphologically assayed gap junctions. Evidence is presented that the peptides at 43,000 and 57,000 are contained within the contaminating *fascia adherens*.

Although both the distribution and ultrastructural appearance of gap junctions have been extensively studied in a wide variety of cell types (7, 15, 32, 36, 38, 40), knowledge of the biochemistry of gap junctions is limited to the junctions in lens (1, 3, 9, 18) and liver (6, 8, 11, 13, 16, 21–23). These studies contain conflicting reports as to the number and molecular weights of the junctional polypeptides and have left unresolved the question of whether gap junctions from different tissues are biochemically similar. To further investigate the biochemical heterogeneity, it clearly would be advantageous to have gap junctions isolated from a variety of other tissues.

We describe a procedure for the isolation of an enriched fraction of gap junctions from mammalian myocardium without the use of exogenous proteases. The ultrastructure and the SDS electrophoretic profiles of the isolated junctions are presented.

MATERIALS AND METHODS

Reagents

The following is a list of reagents used and their sources: Ultrapure sucrose, Coomassie Brilliant Blue R-250 (Schwartz/Mann Div., Becton, Dickinson & Co., Orangeburg, N. Y.); sodium deoxycholate (DOC), phenylmethylsulfonyl fluoride (PMSF), Tris (hydroxymethyl)aminomethane (Sigma Chemical Co., St. Louis, Mo.); Sarkosyl NL-97 (Geigy Industrials, Ardsley, N. Y.); Tween 20 (polyoxyethylene sorbitan monolaurate, ICI United States, Inc., Wilmington, Del.); acrylamide, *N,N*-methylene bis-acrylamide (Eastman Kodak Company, Rochester, N. Y.); sodium lauryl sulfate (Gallard-Schlesinger Chemical MFG Corporation, Carle Place, N. Y.); electrophoresis grade urea (Bio-Rad Laboratories, Richmond, Calif.).

Isolation Procedure

Gap junctions were isolated from the hearts of 49-d-old mice of either sex (Charles River Breeding Laboratories, Inc., Wilmington, Mass.) by a modification of the procedure of Goodenough et al. (19). Unless otherwise noted, all centrifugations were performed at 5°C in either a Beckman J-21C preparative centrifuge or an L5-65 ultracentrifuge (Beckman Instruments, Inc., Spinco Div., Palo Alto, Calif.). In each experiment the hearts from 100 mice (killed by cervical dislocation) were excised, rinsed with cold 1 mM $NaHCO_3$ (pH 8.2) to remove the excess blood, and homogenized in 200 ml of the buffer with a Polytron (Brinkman Instruments, Inc., Westbury, N. Y.) at maximum power for 30 s. The homogenate after dilution to 1,500 ml with 1 mM $NaHCO_3$ was allowed to stand for 10 min on ice to precipitate the released DNA (please refer to Fig. 1). After filtration through 32 layers of cheesecloth, the filtrate was centrifuged (spin 1, 3,700 rpm × 20 min; Beckman JA-14 rotor) and the supernate was removed with a syringe and stored on ice. The pellet was rehomogenized with the Polytron (maximum power × 30 s) in 300 ml of 1 mM $NaHCO_3$, diluted to 1,500 ml, and pelleted again (spin 2, 3700 rpm × 20 min; Beckman JA-14 rotor). The supernate was collected as in spin 1. The pellet after resuspension to 300 ml in 1 mM $NaHCO_3$ was diluted with an equal volume of 1.2 M KI + 12 mM sodium thiosulfate in 1 mM $NaHCO_3$, and the solution was stored on ice. The supernate from spins 1 and 2 were combined and centrifuged (spin 3, 10,000 rpm × 30 min; Beckman JA-10 rotor), giving pellets with light-colored upper portions and reddish-brown-colored lower halves. Small aliquots of 1 mM $NaHCO_3$ were added to each of the pellets, and the centrifuge bottles were gently swirled to resuspend the less firm upper portion of each pellet, which was decanted and discarded. The firmer reddish-brown-colored lower halves of the pellets were resuspended in the 600 ml of buffered KI solution already containing the pellet from spin 2, and the solution was stirred overnight at 4°C. The next morning, the KI-homogenate was pelleted (10,000 rpm × 40 min; Beckman JA-10 rotor); the pellet resuspended in 200 ml of 0.6 M KI + 6 mM sodium thiosulfate in 5 mM Tris buffer, pH 9 (Tris-KI solution); and the solution centrifuged again (12,000 rpm × 30 min; Beckman JA-14 rotor). The pellet of KI-insoluble material was resuspended with the Polytron (1/8 maximum power × 15 s) in 40 ml of Tris-KI solution; sonicated with a Branson ultrasonicator (Branson Instruments Co., Stamford, Conn.) at 0.7 maximum output for 15 s; and the sonicate brought to 50% sucrose by the

addition of 2 vol of 67% sucrose (wt/vol) in Tris-KI solution. 12 sucrose step gradients were prepared by layering 10 ml of the 50% sucrose (plus sample) at the bottom of each tube, followed sequentially by 8 ml each of 45, 35, and 30% sucrose in 5 mM Tris (pH 9) with 1 g of KI and 1.5 mg of sodium thiosulfate added per ml. The gradients were overlaid with 5 ml of Tris-KI solution and were spun for 2 h at 25,000 rpm in Beckman SW 27 rotors. The material floating on the 20% sucrose layer was collected, diluted to 225 ml with 5 mM Tris, and pelleted (25,000 rpm × 30 min; Beckman SW 27 rotor). The pellet of membranes was resuspended in 50 ml of 5 mM Tris (pH 9) with 3 strokes of a type B pestle in a Dounce homogenizer (VirTis Co., Inc., Gardiner, N. Y.) and dialyzed overnight against 6 liters of 5 mM Tris, (pH 9) at 4°C to remove the residual KI. The dialysate was rehomogenized with three strokes in the Dounce homogenizer, diluted to 200 ml with 5 mM Tris (pH 10), and 200 ml of 0.6% Sarkosyl NL-97 in 5 mM Tris (pH 10) was added with stirring at room temperature (23°C). After incubation for 10 min, the solution was centrifuged (10,000 rpm × 40 min at 15°C; Beckman JA-10 rotor) and the pellet resuspended in 20 ml of 0.5% Tween 20 in 5 mM Tris (pH 10). This material was layered on two 43%/30% sucrose (wt/vol) step gradients and the gradients were spun at 25,000 rpm × 1.5 h at 15°C in the SW 27 rotor. The partially purified gap junctions were collected from the 43%/30% interface; diluted to 39 ml with 5 mM Tris (pH 10); and pelleted (25,500 rpm × 30 min; SW 27 rotor). The pellet was resuspended in 2 ml of 5 mM Tris (pH 10), and 37 ml of 0.3% DOC was added with stirring at room temperature. After centrifugation (25,000 rpm × 30 min at 15°C; Beckman SW 27 rotor), the pellet was resuspended in 10 ml of 0.3% DOC and layered on two 43%/30% sucrose (wt/vol) step gradients which were spun at 25,000 rpm × 1.5 h at 15°C in the SW 27 rotor. The band at the 43%/30% interface was collected, diluted to 39 ml with 5 mM Tris (pH 10), and pelleted (25,000 rpm × 30 min, Beckman SW 27 rotor) to give the final fraction of gap junction.

In some experiments, PMSF and parachloromercuribenzoate (PCMB) were added to all solutions at final concentrations of 1 and 2 mM, respectively, to inhibit proteolysis. The PMSF was added fresh every hour to the buffer by adding 1 ml of a 0.1-M solution in absolute alcohol per 100 ml.

Electron Microscopy

NEGATIVE STAINING: Isolated gap junctions were negatively stained on carbon-coated, Formvar-covered grids with aqueous solutions of either 1% uranyl acetate or 1% uranyl formate.

THIN SECTIONING: Pellets from the various stages of the isolation protocol were prepared by centrifugation (40,000 rpm × 1.5 h; Beckman SW 41 rotor) in BEEM hemihyperboloid polyethylene capsules (Ladd Research Industries, Inc., Burlington, Vt.) in Epon centrifuge adaptors (17). The pellets were fixed for 1 h in 5% glutaraldehyde in 0.1 M sodium cacodylate buffer (pH 7.4); rinsed overnight in the cacodylate buffer; and osmicated in 2% osmium tetroxide for 2 h. After en bloc staining with 1% aqueous uranyl acetate, the pellets were dehydrated through a graded ethanol series; infiltrated with a 1:1 mixture of propylene oxide and Epon; and embedded in Epon. Thin sections were stained in 2% uranyl acetate in 50% methanol and for 3 s in Reynolds' lead citrate (37). Cardiac muscle bundles were fixed in 1.5% glutaraldehyde-1.5% paraformaldehyde in 0.15 M cacodylate buffer for 4 h and then osmicated and embedded as for the pellets.

MEASUREMENTS: All specimens were examined in a Siemens 101 electron microscope at 80 kV. For measurement of the junctional widths, all electron micrographs were taken at × 80,000 during a single photographic session. Variations in the instrument magnification were minimized by not varying the magnification between exposures. The magnification was calculated from the repeat spacing (395 Å) of negatively stained tropomyosin tactoids photographed at the same magnification.

SDS Gel Electrophoresis

SDS polyacrylamide slab gel electrophoresis was performed using the discontinuous Tris-glycine buffer system described by Laemmli (27). Slab gels, 1.5 mm thick, were employed with 5% stacking gels and 12.5% separating gels. The sample dissolving buffer contained 62.5 mM Tris-HCl (pH 6.8), 2% (wt/vol) SDS, 12.5% (vol/vol) glycerol, 5% (vol/vol) 2-mercaptoethanol, 0.01% (wt/vol) Bromphenol Blue; with 0.12 g/ml of electrophoreses grade urea added to the final solution. Samples in the dissolving buffer were heated at 50°C for 30 min before loading on the gels. Molecular weights were estimated by reference to standard proteins. These included the myosin heavy chain (200,000), phosphorylase a (95,000), bovine serum albumin (68,000), catalase (60,000), actin (43,000), aldolase (40,000), carbonic anhydrase (29,000), RNase (14,000), and cytochrome *c* (12,000). The gels were stained with Coomassie Brilliant Blue R-250 as described by Fairbanks et al. (14). In some cases, samples were alkylated with iodoacetamide (10) before electrophoresis. For comparison, junctional samples were also electrophoresed on 7.5% polyacrylamide disc gels using the SDS Tris-glycine continuous buffer system described by Stephens (41). Protein concentrations were estimated using the method of Lowry et al. (30), recognizing that these data may be an overestimate of the actual protein concentration (22).

RESULTS

Isolation Procedure

The procedure has been developed for the isolation of gap junctions from mouse myocardium (Fig. 1). The mouse heart, although small in size, is a highly advantageous tissue for the isolation of junctions, because of both size of the junctions (Figs. 2 and 3), and the smaller amounts of collagen between its cells, compared to the hearts of larger mammals.

As illustrated (Figs. 2 and 3), the major cellular components to be removed in isolating the myocardial junctions are the myofibrillar apparatus, mitochondria, the sarcolemmal and sarcoplasmic reticulum membranes, and the desmosomes and *fascia adherens* junctions of the intercalated disc. In the procedure illustrated in Fig. 1, spins 1, 2, and 3 serve primarily to remove the soluble elements of the cytoplasmic matrix and fragments of the sarcoplasmic reticulum in the supernates. Most of the myofibrillar contractile apparatus is then dissolved

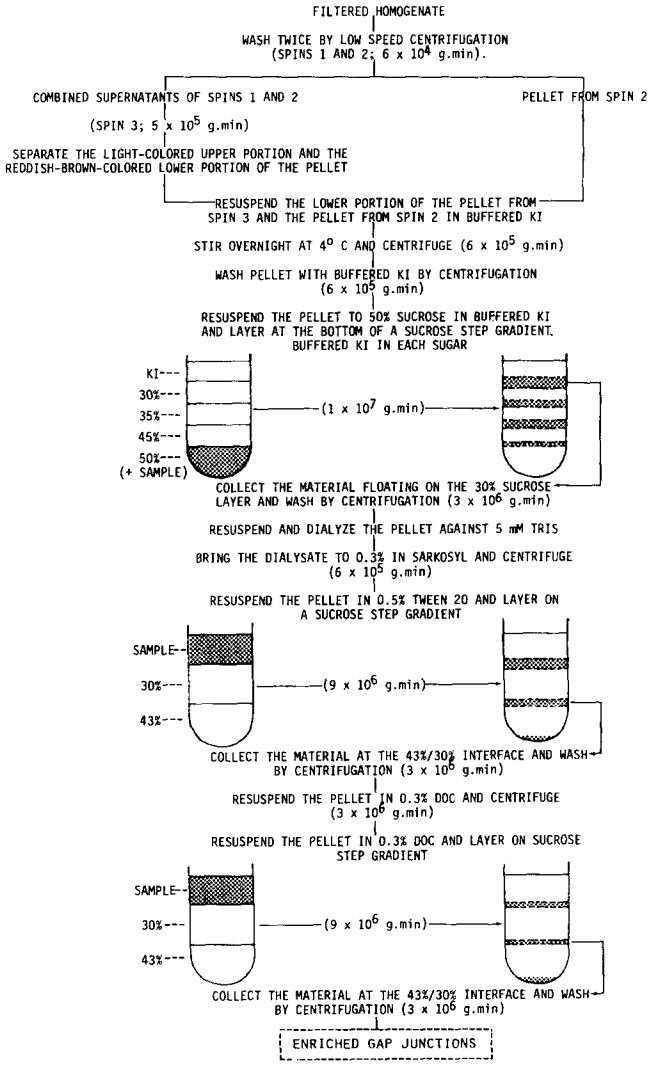

FIGURE 1 A scheme for the isolation of gap junctions from mouse myocardium. Centrifugations are expressed in units of g·min to facilitate the adaptation of the procedure to other rotors and centrifuges. Specific details are given in Materials and Methods.

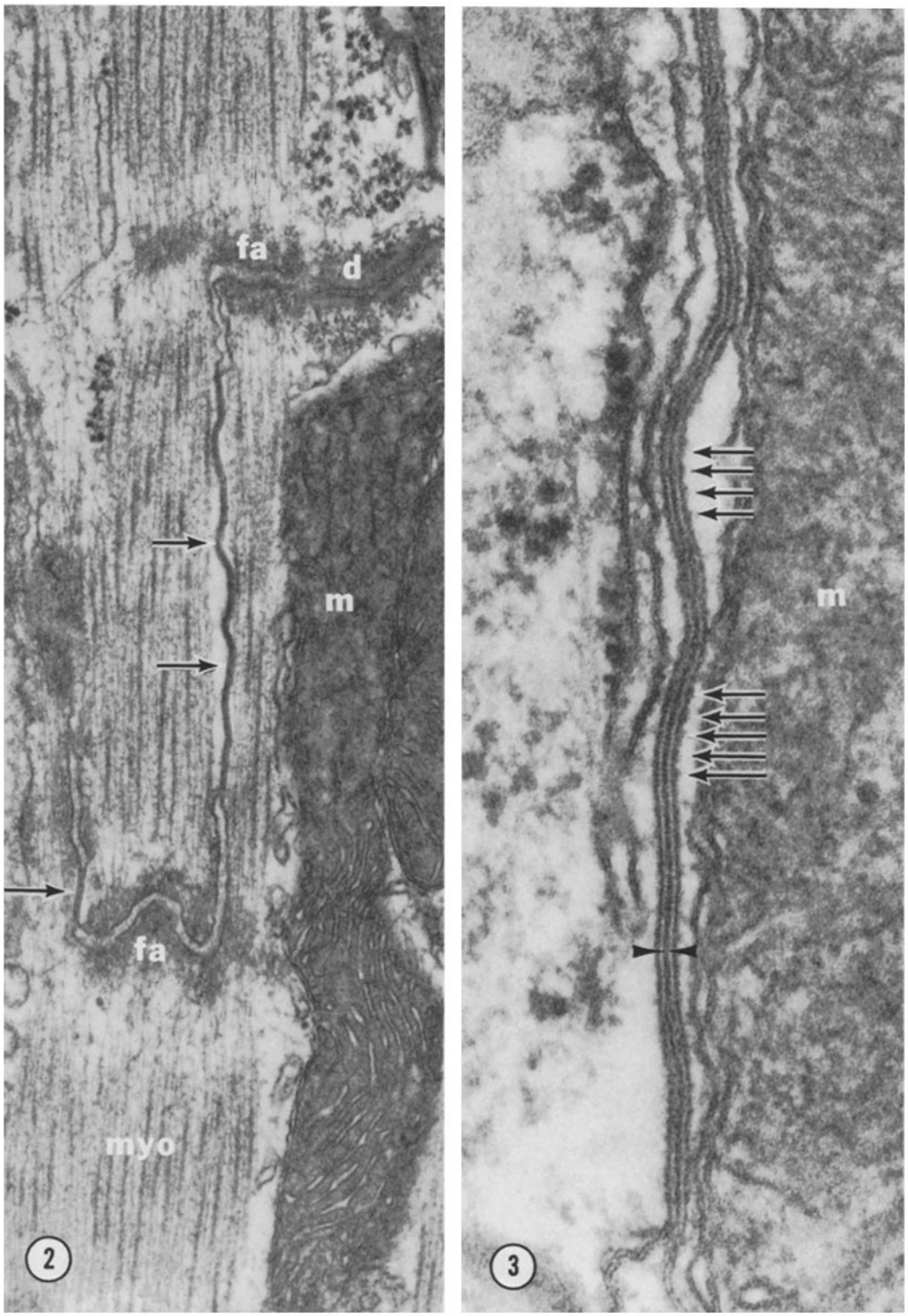

FIGURES 2 and 3 Electron micrographs of thin sections of the *in situ* mouse myocardial junctions. At low magnification (Fig. 2) the variable length of the junctions (arrows) and their frequent close association with the *fascia adherens (fa)* and desmosomes (*d*) of the intercalated disk is apparent. Adjacent structures in the cytoplasm include mitochondria (*m*) and myofibrils (*myo*). At higher magnifications (Fig. 3) the gap junctions appear septilaminar with a 2- to 3-nm electron-translucent gap (apposed arrowheads) between the junctional membranes. Note the frequent periodic appearance of the density along the cytoplasmic surfaces (arrows). Fig. 2: × 56,000. Fig. 3: × 182,000.

by treatment of the remaining homogenate with 0.6 M potassium iodide (KI), leaving a KI-resistant fraction consisting of mitochondrial membranes, fragments of the intercalated disk, sarcolemmal membrane vesicles, and the gap junctions. Fractionation of this KI-resistant material on sucrose gradients containing KI allows a separation of the junctions from a large

fraction of the fragments of the intercalated disk. The junctions and fragments of mitochondrial membrane float on the 30% sucrose-KI layer (ρ = 1.2) while the fragments of the intercalated disc remain at the 35/45% interface (ρ = 1.27) of the sucrose-KI gradient. The inclusion of 0.6 M KI in all of the sugars of the gradient substantially modifies their densities and appears to be important in preventing the clumping of the sample at the interfaces. Subsequent treatment of the material floating on the 30% sucrose-KI layer with 0.3% Sarkosyl followed by 0.5% Tween 20 (Fig. 1) dissolves most of the nonjunctional membranes (see lane 11, Fig. 11), leaving the more detergent-resistant junctions. Higher concentrations of Sarkosyl NL-97 than 0.3–0.35% (wt/vol) tend to dissolve the junctions. Upon fractionation of the Sarkosyl NL-97- and Tween 20-resistant residue on a 43%/30% sucrose step gradient, the partially purified junctions float at the 43%/30% interface while the majority of the remaining fragments of the intercalated disk pellet at the bottom of the gradient. The separation of the fragments of the intercalated disk from the gap junctions on the gradient appears to be facilitated by resuspension of the Sarkosyl-resistant residue in Tween 20 before loading on the gradient. Further treatment of the partially purified junctions with 0.3% DOC (wt/vol) followed by centrifugation on another 43%/30% sucrose step gradient allows solubilization of the remaining nonjunctional membranes and a pelleting of additional fragments of the intercalated disk at the bottom of the gradient. The purified gap junctions are recovered floating at the 43%/30% interface (Figs. 4 and 5).

In initial experiments (26), the myocardial junctions were isolated solely from the pellet of the homogenate after low-speed centrifugation (spins 1 and 2 in Fig. 1), thus allowing an early removal of most of the mitochondrial and sarcoplasmic reticulum membranes in the supernates. Subsequent experiments, however, revealed that large numbers of junctions were also being lost in the supernates. Simply centrifuging the homogenate at higher speeds or for longer times to pellet all of the junctions resulted in a final junctional preparation that was grossly contaminated with detergent-resistant fibrillar debris. It was determined empirically, however, that if the supernates from spins 1 and 2 (Fig. 1) were combined and centrifuged (5×10^5 g·min, spin 3), a two-layered pellet resulted with most of the junctions in the lower half of the pellet and most of the detergent-resistant contaminants in the upper half of the pellet. By discarding the upper half of this pellet and combining the lower half with the pellet from the low-speed spins (spins 1 and 2), the yield of junctions in the final preparation can be substantially increased with little additional contamination of the preparation. The final yield of the procedure is typically 50–150 μg of protein from an initial 16 μg of heart (wet weight).

Morphology of the Isolated Gap Junctions

In thin sections, the isolated preparation appears highly enriched for gap junctions of variable length (Figs. 4 and 5), which are present as both flat sheets and vesicular profiles in proportions that vary from run to run. The main contaminants of the preparation are fragments of the *fascia adherens* region of the intercalated disk and occasional small amorphous contaminants of unknown origin (Fig. 4), both of which may be present to variable degrees in different preparations.

At higher magnifications (Fig. 5), the appearance of the isolated gap junctions in thin sections is similar to that *in situ* (compare Figs. 3 and 5). The isolated junctions appear septilaminar, with retention of the 2- to 3-nm electron-translucent gap between the junctional membranes (Fig. 5). Treatment with the detergent DOC at a concentration of 0.3 mg/ml did not cause the collapse of the gap region of the junction. The width of the isolated junctions (18.7 ± 1.6 nm, n = 325 measurements; 47 junctions) is not significantly different from that of the *in situ* junctions (19.1 ± 1.2 nm, n = 115 measurements; 19 junctions). The isolated junctions retain the enhanced density along their cytoplasmic surfaces (Fig. 5) which is characteristic *in situ* (Fig. 3). In many places the density along the cytoplasmic surfaces of the junction appears periodic (Figs. 3 and 5).

Upon negative staining, the isolated junctions appear both as flat sheets and as collapsed vesicles (Figs. 6 and 7). The negatively stained double-membrane profile of the junction can be seen at the edges of the vesicles and at folded-over regions of the flat sheets (arrow, Fig. 6). In these regions the junction appears as a stain-filled gap separating a pair of stain-excluding junctional membranes. Holes and other discontinuities in the junctional plaques occur only infrequently.

At higher magnification (Fig. 7), a polygonal array of 6- to 7-nm diameter subunits (connexons) similar to that observed in isolated liver and brain gap junctions (2, 5, 16, 22, 23, 43) is delineated by the negative stain. Although the connexons in many regions of the junctions appear hexagonally packed with a center-to-center spacing of 9–10 nm (Fig. 7), long-range lattice order is usually absent. The degree of lattice order appears to be variable from preparation to preparation, for reasons that are not known. A 1- to 2-nm diameter electron-dense region is apparent at the center of each connexon (Fig. 7) after negative staining with uranyl formate. Uranyl acetate also delineates this density, but usually with less clarity.

SDS Polyacrylamide Gel Electrophoresis

An SDS slab gel electrophoretic analysis of the fractions at various stages in the isolation of the myocardial gap junction is illustrated in Fig. 8. The removal of most of the contractile proteins by 0.6 M KI (lane 4) and of the majority of the remaining polypeptides by Sarkosyl NL-97 and Tween 20 (lane 9) is apparent. In the final junction-enriched preparation (lanes 10 and 11), seven major bands are typically present with apparent mol wt of 28,000, 31,000, 33,500, 43,000, 47,000, and 57,000. In gels heavily loaded with protein, a number of minor bands of higher molecular weight are also frequently revealed. Bands of molecular weight lower than 28,000, such as might be generated by proteolysis, are seldom apparent (lanes 10 and 11). The alkylation of the samples with iodoacetamide (10) before electrophoresis or the inclusion of the proteolytic inhibitors PMSF and PCMB in all of the solution during the isolation procedure does not modify the polypeptide profile. Nor does the polypeptide profile seem to depend upon whether the junctions are primarily in the form of flat sheets or vesicles.

Electrophoresis of the enriched preparation of junctions on tube gels (7.5% acrylamide) using the continuous SDS Tris-glycine buffer system of Stephens (41) gives a similar polypeptide profile (data not shown), except that the members of the triplet at 28,000, 31,000, and 33,500 are usually not well resolved from each other and appear as a single broad band as reported previously (26).

Of the major bands in the final preparation (Fig. 8, lanes 10 and 11), only the triplet at 28,000, 31,000, 33,500, and possibly the diffuse band at 47,000 show a quantitative enrichment

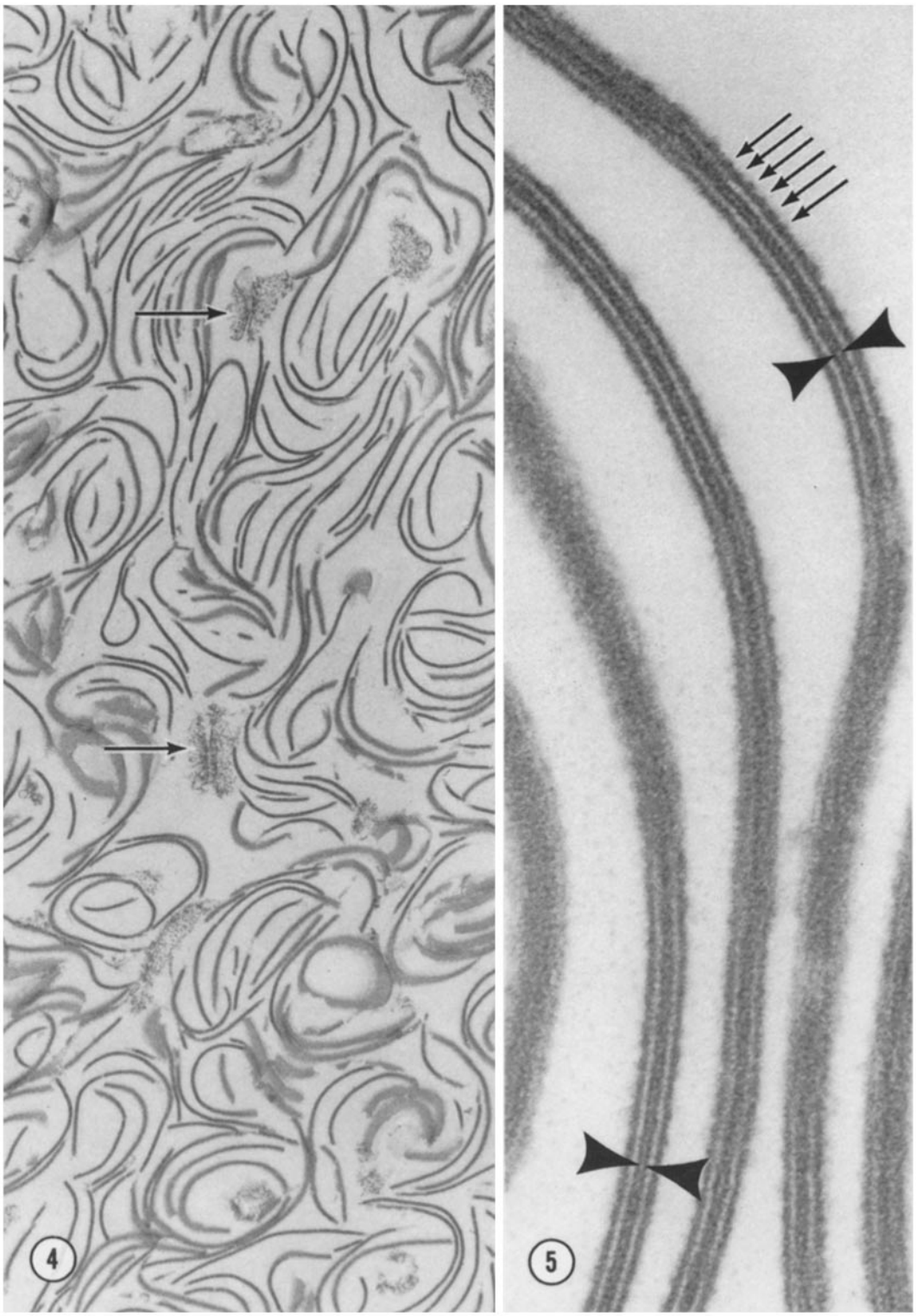

FIGURES 4 and 5 Electron micrographs of thin sections through a high-speed pellet of the enriched preparation of gap junctions. At low magnifications (Fig. 4) the enrichment of the preparation is apparent. Fragments of the *fascia adherens* region of the intercalated disk (arrows) appear to be the major contaminants of the preparation. At higher magnification (Fig. 5) the isolated gap junctions appear septilaminar and similar to their *in situ* appearance. The 2- to 3-nm wide electron-translucent gap between the junctional membranes is apparent in most regions (apposed arrowheads). Note the frequent periodic appearance (arrows) of the density on the cytoplasmic surfaces. Fig. 4: × 28,000. Fig. 5: × 360,000.

concomitant with morphological enrichment of the gap junctions. The bands at 43,000, 49,000, 57,000, and many of the minor high molecular weight bands, in contrast, are most prominent in several of the crude fractions, particularly the 45%/35% interface of the sucrose-KI gradient (Fig. 8, lane 7; Fig. 11, lane 1) and the pellet at the bottom of the sucrose

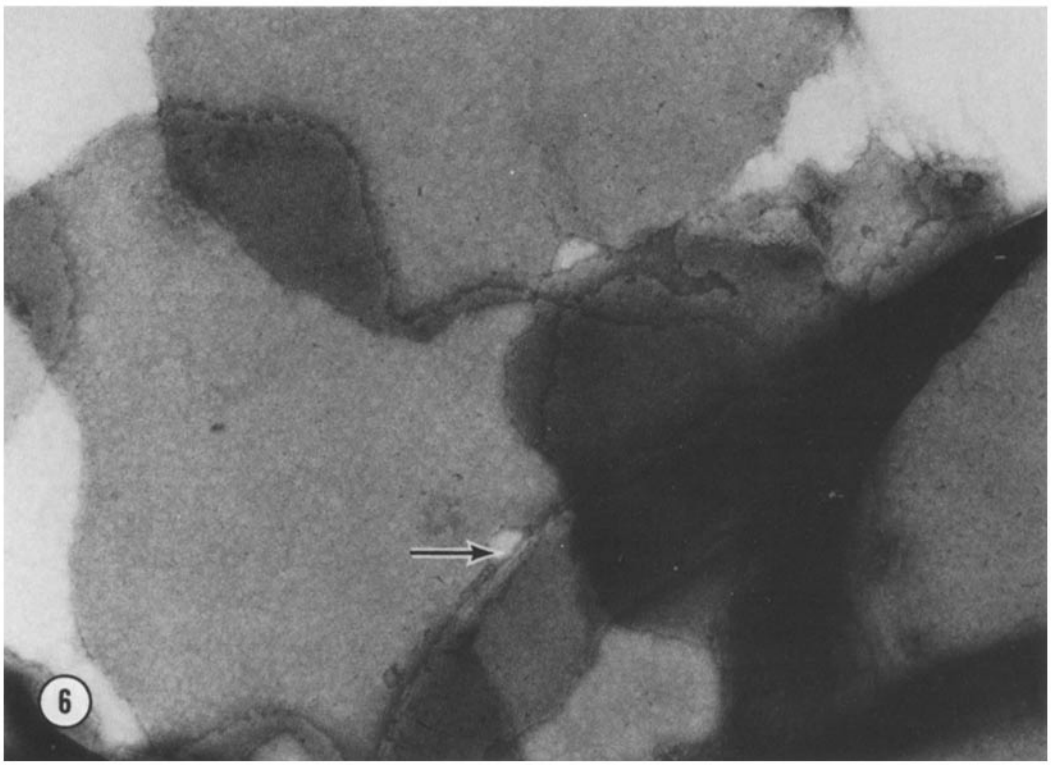

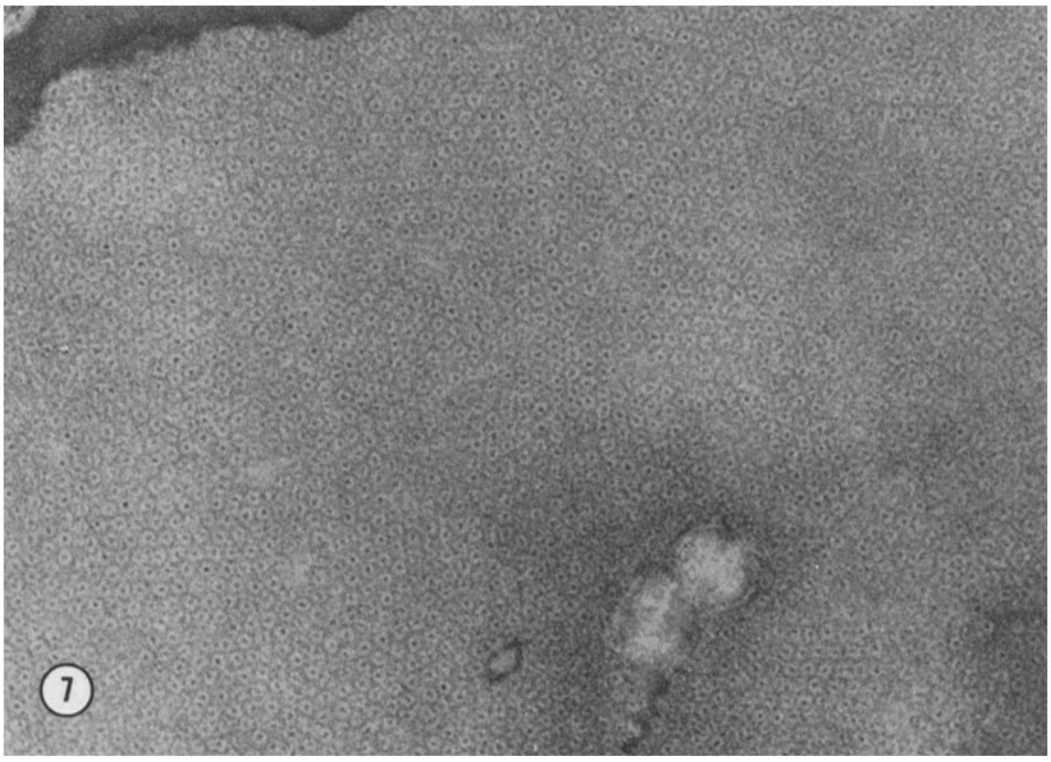

FIGURES 6 and 7 Electron micrographs of the isolated gap junctions negatively stained with 1% uranyl formate. At low magnification (Fig. 6) the junctions appear both as flattened sheets and as broken vesicles. The double-membrane profile of the junction is evident at the edges of the broken vesicles (arrow). At higher magnification (Fig. 7) the closely packed array of connexons is clearly evident. There is a densely staining region in the center of each connexon. Note that the connexons in some regions appear to be hexagonally arranged. Fig. 6: × 67,000. Fig. 7: × 333,000.

gradient immediately after the Sarkosyl NL-97 and Tween 20 treatment of the sample (Fig. 8, lane 8). Examination of the crude fractions by electron microscopy (Figs. 9 and 10) demonstrates that fragments of the *fascia adherens* comprise a major component, suggesting that the polypeptides with mol wt of 43,000, 49,000, and 57,000 may be components of the *fascia adherens* junctions.

To examine this point more closely, an attempt was made to

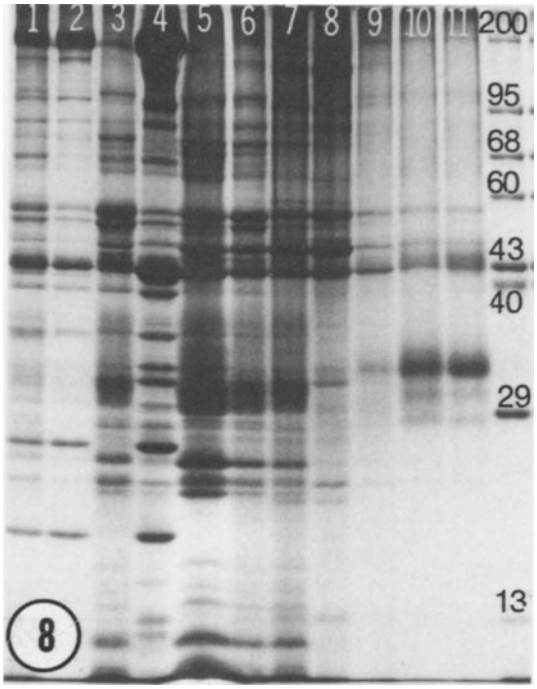

FIGURE 8 SDS polyacrylamide slab gel analysis of various fractions obtained during the purification of the myocardial gap junctions. Lane *12*: the reference proteins. The molecular weights in kilodaltons are indicated. Lane 1: the initial homogenate of the hearts. Lane 2: the pellet from spin 2. Lane 3: the lower portion of the pellet from spin 3. Lane 4: the 0.6 M KI extract. Lane 5: the material at the 30% sucrose/0.6 M KI interface of the sucrose-KI gradient. Lane 6: the material at the 35%/30% interface of the sucrose-KI gradient. Lane 7: the material at the 45%/35% interface of the sucrose-KI gradient. Lane 8: the pellet at the bottom of the post-Sarkosyl/Tween 20 sucrose gradient. Lane 9: the material at the 43%/30% interface of the post-Sarkosyl/Tween 20 sucrose gradient. Lanes *10* and *11*: two different enriched preparations of the gap junctions; from the 43%/30% interface of the post-DOC sucrose gradient.

further purify the intercalated disk fragments. The material at the 45%/35% interface of the sucrose-KI gradient was centrifuged on an additional sucrose step gradient (50%/43%) either with or without prior treatment of the sample with 0.3% Sarkosyl NL-97. Examination of the material at the 50%/43% interface of the gradients of both the Sarkosyl- and non-Sarkosyl-treated samples and of the pellet at the bottom of the gradient of the sarkosyl-treated sample revealed enriched fractions of *fascia adherens* fragments (Fig. 10), with only very minor contamination with gap junctions. Electrophoresis of the gradient fractions (Fig. 11) revealed prominent bands at 43,000 and 57,000 in all of the fractions, thus supporting the conclusion that these bands in the SDS electrophoretic profile of the gap junction preparation (Fig. 8, lanes 10 and 11) correspond to the contaminating fragments of *fascia adherens*, and not to the gap junctions. The band at 49,000, in contrast, did not appear as prominent in the more enriched fractions of *fascia adherens* (Fig. 11, lanes 3–6), and thus may not correspond to the fragments of *fascia adherens*.

DISCUSSION

The isolation procedure described in this paper yields a small quantity of relatively pure gap junctions from mouse myocardium. In contrast to an earlier method (19) for the isolation of myocardial junctions, the present procedure avoids the use of exogenous proteases and gives a morphologically cleaner preparation. The increase in purity is mainly caused by the inclusion of a sucrose step gradient containing KI in the procedure and by the use of Tween 20 and Sarkosyl NL-97. The myocardial gap junctions show an intermediate resistance to sarkosyl solubilization, being less resistant than liver junctions (13, 21) and more resistant than lens fiber gap junctions (18).

The myocardial junctions isolated here appear well preserved by morphological criteria both in thin sections and by negative staining. Although similar to isolated liver gap junctions in their septilaminar appearance (5, 16, 21, 23), the isolated myocardial junctions differ in their greater width and more disordered connexon lattice. The greater width of the myocardial junctions (18.5–19 nm) compared to the width of liver junctions (15–16 nm [20, 21]) has previously been reported (19, 32) and is caused by an increased density along the cytoplasmic surfaces of the myocardial junctions (Figs. 3 and 5) both isolated and *in situ*. An enhanced density along the cytoplasmic surfaces has also been reported for the gap junctions in vertebrate cerebellum (39) and frog myocardium (25), and appears to be present in the gap junctions of smooth muscle illustrated by Uehara and Burnstock (42). Although the significance of this density is not clear, the tissue distribution suggests that it may be a characteristic property of vertebrate gap junctions that act as electrotonic synapses.

In negatively stained preparations, the tightness and orderliness of the packing of the connexons in the isolated myocardial junctions appears to be intermediate between the highly disordered packing in the lens fiber junctions (18, 19) and the more highly ordered packing of the connexons in the liver junctions (5, 22, 31). At present it is not clear to what extent this difference in the packing of the connexons represents an intrinsic difference in the properties of the connexons of these junctions and to what extent it represents the differences in the isolation procedures. That the specific isolation conditions for the junctions may have considerable influence on the arrangement of the connexons is illustrated by the effects of calcium chelators reported by Zampighi and Robertson (43), and by the growing body of evidence that exists for polymorphism in the arrangement of the connexons from a variety of tissues (4, 5, 33–35), depending upon the experimental conditions.

The isolation of gap junctions from liver and lens has resulted in conflicting reports in the literature both as to the number and the molecular weight of the component polypeptides (reviewed in references 22 and 23). Recent studies have revealed that the exogenous proteases used in earlier procedures (16, 21) degrade the junctional proteins (22, 23). Evidence for the heat-induced aggregation of the junctional polypeptides of liver junctions has also been demonstrated and suggested to be a factor in the variations in the SDS electrophoretic profiles of the junctions (22). In the procedure described here, we have avoided the use of exogenous proteases, and have found that the addition of proteolytic inhibitors during the procedure has no effect on the polypeptide profile. The incubation of the sample in SDS at room temperature or at 100°C rather than at 50°C also does not modify the protein electrophoretic profile, thus suggesting that heat-induced aggregation of the junctional polypeptides is probably not occurring.

In comparison with those of lens and liver, the myocardial junctions appear to be unique in the consistent presence of three associated polypeptides with apparent mol wt of 28,000, 31,000, and 33,500. A polypeptide with a mol wt of 47,000 may

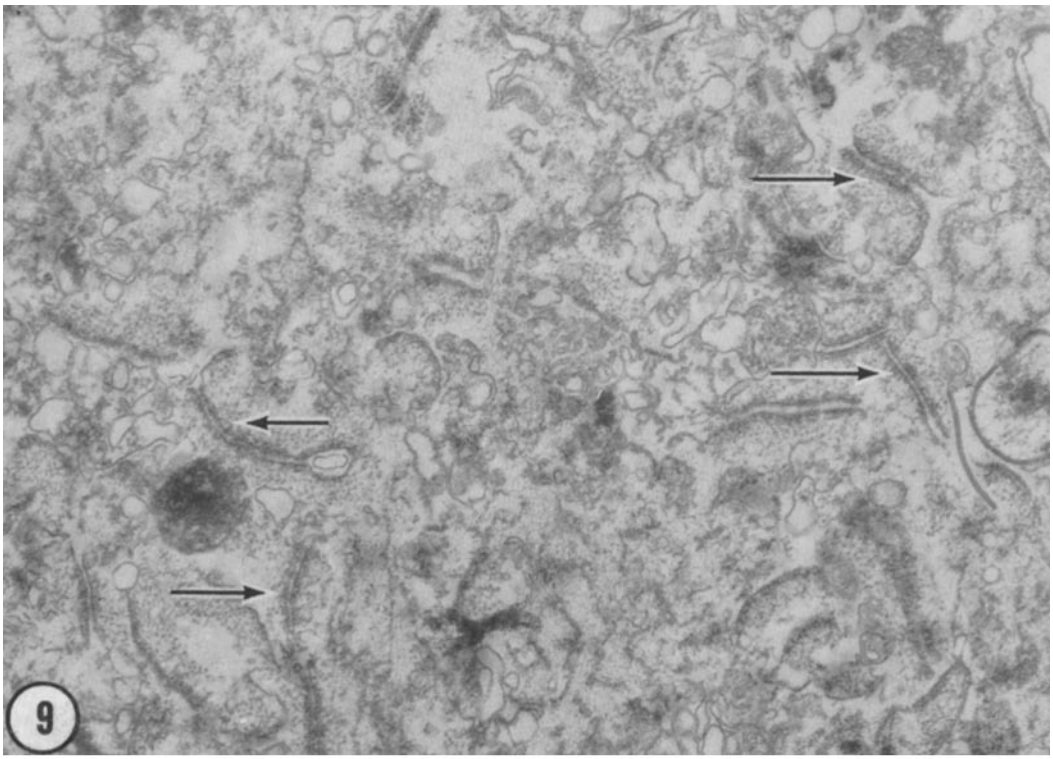

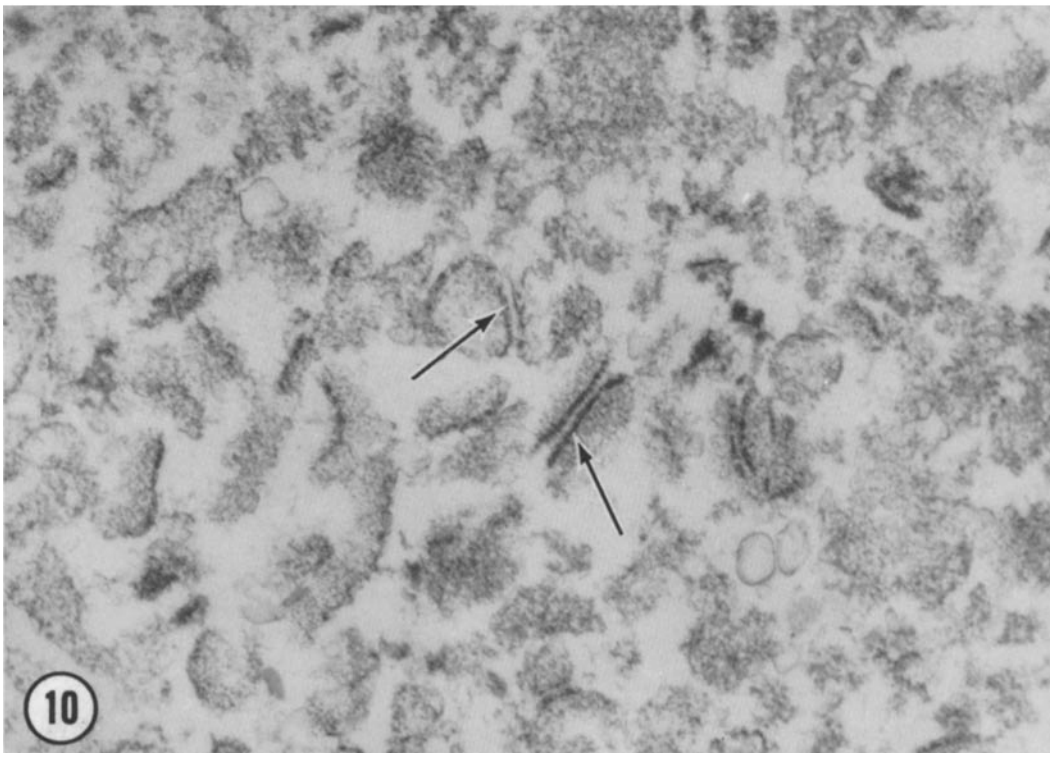

FIGURES 9 and 10 Thin sections of pellets of the material at the 45%/35% interface of the sucrose-KI gradient (Fig. 9) and of the pellet at the bottom of the post-Sarkosyl/Tween 20 sucrose gradient (Fig. 10). Fragments of *fascia adherens* (arrows) are the predominant recognizable components in each fraction. Fig. 9: × 39,000. Fig. 10: × 40,000.

also be associated, but this is less clear because this polypeptide is not always seen. The presence of a band at 34,000, and less frequently a band at 31,000, has been reported for both liver (8, 11) and lens gap junctions (9) on SDS polyacrylamide gels, but these bands have not consistently been observed by all investigators (13, 16, 18, 22, 23). Recent investigations of gap junctions isolated without exogenous proteases have reported mol wt of 27,000 and 47,000 for rat liver (23), 21,000 and 26,000 for mouse liver (22), and 27,000 for the major polypeptide of lens fiber gap junctions (18). The reasons for the variations in the polypeptide profiles reported by different investigators for gap junctions isolated from the same tissue are at present still unclear.

Although exogenous proteolysis is controlled in these pro-

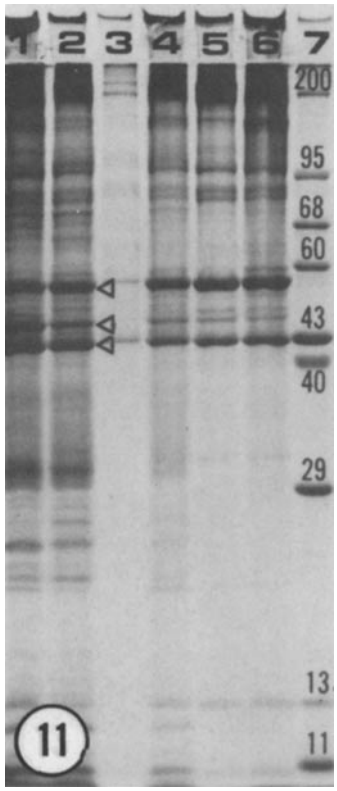

FIGURE 11 SDS polyacrylamide slab gel analysis of fractions obtained in the enrichment for fragments of the *fascia adherens*. The material at the 45%/35% interface of a sucrose-KI gradient was washed and layered on a 50%/43% sucrose step gradient either with or without prior treatment with 0.3% Sarkosyl. After centrifugation the interfaces were examined by electron microscopy and electrophoresis. Lane 1: the starting material at the 45%/35% interface of the sucrose-KI gradient (Fig. 9). Lane 2: the material floating on the 43% layer of the gradient; non-Sarkosyl treated. Lane 3: the material floating on the 43% layer of the gradient; Sarkosyl treated. Lane 4: the 50%/43% interface of the gradient; non-Sarkosyl treated. Lane 5: the 50%/43% interface of the gradient; Sarkosyl-treated. Lane 6: the pellet at the bottom of the gradient of the Sarkosyl-treated sample (Fig. 10). Lane 7: the reference proteins; the molecular weights in kilodaltons are indicated. The arrowheads indicate the positions of the bands with molecular weights of 43,000, 49,000, and 57,000.

tocols, the possibility still remains that rapid, postmortem endogenous proteolysis may occur, and may even be a physiological mechanism for junction regulation. Comparison of junctional peptides from different tissue sources must therefore await more critical peptide mapping. The morphology, detergent solubility, and one-dimensional electrophoretic patterns of heart, liver, and lens fiber gap junctions are nonetheless unique properties that may be reflected in different protein compositions.

Two quantitatively major polypeptides with mol wt of 43,000 and 57,000 appear to copurify with the fragments of the *fascia adherens* region of the intercalated disk. A third polypeptide with a mol wt of 49,000 may also be associated with the fragments. The polypeptides with mol wt of 49,000 and 57,000 are similar in molecular weight to the molecules desmin and skeletin (12, 28, 29) which have been reported to be associated with the intercalated disk and desmosomes. Both of these molecules have been suggested as possible components of the 10-nm filaments (12, 24, 28, 29). The band at 43,000 has an electrophoretic mobility similar to the actin standard on the gels. Hubbard and Lazarides (24) have shown that a fraction of actin that is relatively insoluble in 0.6 M KI is closely associated with desmin. Because desmin is thought to be present at the intercalated disk (29), the associated presence of actin with the disk is not surprising.

The expert technical assistance of Mr. Kenneth Culbert is gratefully acknowledged.

This research is supported by grant-in-aid 76-653 from the American Heart Association, grant GM18974 from the National Institutes of Health (NIH), and grant PCM77-13955 from the National Science Foundation. D. A. Goodenough is supported by RCDA GM00231 from NIH.

Received for publication 17 December 1979, and in revised form 1 May 1980.

REFERENCES

1. Benedetti, E., I. Dunia, C. Bentzel, A. Vermorken, M. Kibbelaar, and H. Bloemendal. 1976. A portrait of plasma membrane specialization in eye lens epithelium and fibers. *Biochim. Biophys. Acta* 457:353–384.
2. Benedetti, E., and P. Emmelot. 1968. Hexagonal array of subunits in tight junctions separated from isolated rat liver plasma membranes. *J. Cell Biol.* 38:15–24.
3. Bloemendal, H., A. Zweers, F. Vermovken, I. Dunia, and E. Benedetti. 1972. The plasma membrane of eye lens fibers. Biochemical and structural characterization. *Cell Differ.* 1: 91–106.
4. Brink, P., R. W. Kensler, and M. M. Dewey. 1979. The effect of lanthanum on the nexus of the anterior byssus retractor muscle of *Mytilus edulis* L. *Am. J. Anat.* 154:11–26.
5. Caspar, D. L. D., D. A. Goodenough, L. Makowski, and W. C. Phillips. 1977. Gap junction structures. I. Correlated electron microscopy and x-ray diffraction. *J. Cell Biol.* 74:605–628.
6. Culvenor, J. G., and W. H. Evans. 1977. Preparation of hepatic gap (communicating) junctions. Identification of the constituent polypeptide subunits. *Biochem. J.* 168:475–481.
7. Dewey, M. M., and L. Barr. 1964. A study of the structure and distribution of the nexus. *J. Cell Biol.* 23:553–585.
8. Duguid, J. R., and J. P. Revel. 1975. The protein components of the gap junction. *Cold Spring Harbor Symp. Quant. Biol.*, 40:45–47.
9. Dunia, I., C. Sen Ghosh, E. L. Benedetti, A. Zweers, and H. Bloemendal. 1974. Isolation and protein pattern of eye lens fiber junctions. *FEBS (Fed. Eur. Biochem. Soc.) Lett.* 45: 139–144.
10. Dwyer, N., and G. Blobel. 1976. A modified procedure for the isolation of pore complex-lamina fraction from rat liver nuclei. *J. Cell Biol.* 70:581–591.
11. Ehrhart, J. C., and J. Chauveau. 1977. The protein component of mouse hepatocyte gap junctions. *FEBS (Fed. Eur. Biochem. Soc.) Lett.* 78:295–299.
12. Eriksson, A., and L. E. Thornell. 1979. Intermediate (skeleton) filaments in heart Purkinje fibers. A correlative morphological and biochemical identification with evidence of a cytoskeletal function. *J. Cell Biol.* 80:231–247.
13. Evans, W. H., and J. W. Gurd. 1972. Preparation and properties of nexuses and lipid enriched vesicles from mouse liver plasma membrane. *Biochem. J.* 128:691–699.
14. Fairbanks, G., T. L. Steck, and D. F. H. Wallach. 1971. Electrophoretic analysis of the major polypeptides of the human erythrocyte membrane. *Biochemistry.* 10:2606–2617.
15. Gilula, N. B. 1974. Junctions between cells. *In Cell Communication.* R. P. Cox, editor. John Wiley and Sons, New York. 1–29.
16. Goodenough, D. A. 1974. Bulk isolation of mouse hepatocyte gap junctions. Characterization of the principal protein, connexin. *J. Cell Biol.* 61:557–563.
17. Goodenough, D. A. 1975. Methods for the isolation and structural characterization of hepatocyte gap junctions. In: *Methods in Membrane Biology.* E. D. Korn, editor. Plenum Press, New York. 3:51–80.
18. Goodenough, D. A. 1979. Lens gap junctions: a structural hypothesis for non-regulated low resistance intercellular pathways. *Invest. Ophthalmol. Visual Sci.* 18:1104–1122.
19. Goodenough, D. A., D. L. Paul, and K. E. Culbert. 1978. Correlative gap junction ultrastructure. *In* Birth Defects: Original Article Series. 14 (No. 2):83–97.
20. Goodenough, D. A., and J. P. Revel. 1970. A fine structural analysis of intercellular junctions in the mouse liver. *J. Cell Biol.* 45:272–290.
21. Goodenough, D. A., and W. Stoeckenius. 1972. The isolation of mouse hepatocyte gap junctions. Preliminary chemical characterization and x-ray diffraction. *J. Cell Biol.* 54: 646–656.
22. Henderson, D., H. Eibl, and K. Weber. 1979. Structure and biochemistry of mouse hepatic gap junctions. *J. Mol. Biol.* 132:193–218.
23. Hertzberg, E. L., and N. B. Gilula. 1979. Isolation and characterization of gap junctions from rat liver. *J. Biol. Chem.* 254:2138–2147.
24. Hubbard, B. D., and E. Lazarides. 1979. Copurification of actin and desmin from chicken smooth muscle and their copolymerization *in vitro* to intermediate filaments. *J. Cell Biol.* 80:166–182.
25. Kensler, R. W., P. Brink, and M. M. Dewey. 1977. Nexus of frog ventricle. *J. Cell Biol.* 73: 768–781.
26. Kensler, R. W., and D. A. Goodenough. 1978. Isolation of the nexus from mouse myocardium. *Circulation.* 58:II–53.
27. Laemmli, U. K. 1970. Cleavage of structural proteins during the assembly of the head of bacteriophage T4. *Nature (Lond.).* 227:680–685.
28. Lazarides, E. 1978. The distribution of desmin (100 A) filaments in primary cultures of embryonic chick cardiac cells. *Exp. Cell Res.* 112:265–273.
29. Lazarides, E., and B. D. Hubbard. 1976. Immunological characterization of the subunit of the 100 A filaments from muscle cells. *Proc. Natl. Acad. Sci. U. S. A.* 73:4344–4348.
30. Lowry, O. H., N. J. Rosebrough, A. L. Farr, and R. J. Randall. 1951. Protein measurement with the Folin phenol reagent. *J. Biol. Chem.* 193:265–275.
31. Makowski, L., D. L. D. Caspar, W. C. Phillips, and D. A. Goodenough. 1977. Gap junction structures. II. Analysis of the x-ray diffraction data. *J. Cell Biol.* 74:629–645.
32. McNutt, N. S., and R. S. Weinstein. 1970. The ultrastructure of the nexus. A correlated

thin-section and freeze-cleave study. *J. Cell Biol.* 47:666–688.
33. Peracchia, C. 1977. Gap junctions. Structural changes after uncoupling procedures. *J. Cell Biol.* 72:628–641.
34. Peracchia, C., and A. F. Dulhunty. 1976. Low resistance junctions in crayfish. Structural changes with functional uncoupling. *J. Cell Biol.* 70:419–439.
35. Raviola, E., D. A. Goodenough, and G. Raviola. 1978. The native structure of gap junctions rapidly frozen at 4°K. *J. Cell Biol.* 79 (2, Pt. 2):229*a* (Abstr.).
36. Revel, J. P., and M. J. Karnovsky. 1967. Hexagonal array of subunits in intercellular junctions of the mouse heart and liver. *J. Cell Biol.* 33:C7.
37. Reynolds, E. 1963. The use of lead citrate at high pH as an electron-opaque stain in electron microscopy. *J. Cell Biol.* 17:208–212.
38. Satir, P., and N. B. Gilula. 1973. The fine structure of membranes and intercellular communication in insects. *Annu. Rev. Entomol.* 18:143–166.
39. Sotelio, C., and R. Llinas. 1972. Specialized membrane junctions between neurons in the vertebrate cerebellar cortex. *J. Cell Biol.* 53:271–289.
40. Staehelin, L. A. 1974. Structure and function of intercellular junctions. *Int. Rev. Cytol.* 39: 191–283.
41. Stephens, R. E. 1975. High resolution preparative SDS polyacrylamide gel electrophoresis: fluorescent visualization and electrophoretic elution-concentration of protein bands. *Anal. Biochem.* 65:369–379.
42. Uehara, Y., and G. Burnstock. 1970. Demonstration of "gap junctions" between smooth muscle cells. *J. Cell Biol.* 44:215–217.
43. Zampighi, G., and J. D. Robertson. 1973. Fine structure of the synaptic discs separated from the goldfish medulla oblongata. *J. Cell Biol.* 56:92–105.